The role of dynamic sea ice in a simplified general circulation model used for paleoclimate studies

Moritz Adam[*1], **Heather J. Andres**[2] **and Kira Rehfeld**[1,3]

[1] Institute of Environmental Physics, Heidelberg University
Heidelberg, Germany

[2] Memorial University of Newfoundland
St. John's, NL, Canada

[3] Geo- und Umweltforschungszentrum, Eberhard Karls Universität Tübingen
Tübingen, Germany

[*] Correspondence: Moritz Adam (madam@iup.uni-heidelberg.de)

Key words: Climate Modelling, Sea Ice Dynamics, Paleoclimatology

Abstract: *Observational records provide a strong basis for constraining sea ice models within a narrow range of climate conditions. Given current trends away from these conditions, models need to be tested over a wider range of climate states. The past provides many such examples based on paleoclimate data, including abrupt, large-amplitude climate events. However, the millennial-duration of typical paleoclimate simulations necessitates balancing the inclusion and sophistication of model processes against computational cost. This is why many simplified models used for multi-millennial simulation only feature representations of thermodynamic sea ice processes, while representing sea ice dynamics is essential for more complex general circulation models. We investigate the impact on climate mean states and variability of introducing sea ice dynamics into the simplified general circulation model PlaSim-LSG.*

We extend the default thermodynamic sea ice component in PlaSim-LSG with one that includes also dynamic sea ice processes. We adapt the structure and parallelization scheme of this new submodel originating from the MITgcm, a more complex state–of–the–art general circulation model. Then, we evaluate the impact of sea ice dynamics on the simulated climate. Comparing climatologies and the variability of the extended model to control simulations of the pre-existing setup, we find that the standard model overestimates sea ice extent, concentration and thickness. The extended model, however, is biased towards low sea ice amounts and extent. Modifying individual parameters in initial tests of the newly added component is not sufficient to compensate for this bias. Still, the general ability of the model to represent positive and negative biases of the sea ice cover provides a promising starting point for the tuning of PlaSim-LSG with sea ice dynamics. Eventually, the extended model can be used to investigate the role of sea ice for past climate oscillations.

1 INTRODUCTION

Paleoclimate simulations provide a test-bed to constrain climate models of different complexity over a much wider range than what is available from instrumental records [1, 2]. In addition, they provide an opportunity to verify concepts on mechanisms and tipping elements which led to abrupt climate oscillations in the past. Sea ice is closely linked with past abrupt climate transitions as found in model studies [3–6] and inferred from paleoclimate archives [7, 8].

A major limitation of transient paleoclimate simulations over multiple millennia with state–of–the–art general circulation models (GCMs), which represent the earth system to a great level of detail, are the high computational costs. Simplified GCMs still offer a reasonable representation of the atmosphere and ocean with a dynamical atmospheric core and a mixed-layer

https://doi.org/10.4995/YIC2021.2021.12383

or dynamic ocean component [9]. Depending on the questions and time scales of interest, they additionally feature representations of other components of the earth system, like sea ice thermodynamics or simple vegetation [10]. Yet, simplified GCMs are typically highly parametrized, have a relatively coarse spatial resolution to allow for moderate computational cost in simulations of multiple millennia, and are often specifically adapted to answer specific research questions with design decisions carefully weighing model complexity against computational costs [9–12]. As a result, simplified GCMs or models of intermediate complexity do not take all earth system processes into account in great detail and, other than in more complex state–of–the–art general circulation models, it is not always common to, for example, model the dynamics of sea ice. Simplified GCMs can, however, help to build a better understanding about which processes are actually needed to effectively resolve particular climate phenomena [11].

The Planet Simulator (PlaSim) [13–15] coupled to the Large Scale Geostrophic Ocean (LSG) [16] is a well-studied simplified GCM. It solves the primitive equations in the atmosphere, approximates the dynamical equations of the ocean under the assumptions of large spatial and temporal scales, and employs simplified parametrisations for processes like sea ice thermodynamics, greenhouse gas forcing, and land cover and vegetation [14]. However, it does not contain a component to model the dynamics of sea ice up to this point. PlaSim and its atmospheric core PUMA have been used in a wide range of applications from synchronization experiments [17] to entropy and hysteresis studies [18]. More recently, the model was used to study the dynamical landscape of climate [19] and in combination with LSG in a study on atmospheric contributions to abrupt climate changes in the past [20]. LSG has been extensively studied and was a part of CMIP1 [21] and of Paleoclimate Model Intercomparison Projects [e.g. 22–24].

Yet, it has been shown that under climate conditions of the Last Glacial Maximum, the time period of greatest land-based ice volume during the Last Glacial period, occuring around 21 kyr ago [25], PlaSim-LSG has pronounced biases with respect to CMIP5 simulations towards too low high-latitude winter temperatures over oceanic and snow-covered land regions [20]. Similar biases occur under present-day conditions during winter in high latitudes. The model overestimates climate sensitivity as is visible from transient simulations [26, 27] and simulates unrealistically large and thick amounts of sea ice. Dynamics of sea ice are crucial to realistically represent the sea ice thickness distribution, while sea ice thermodynamics are most relevant to enable feedbacks with earth system compartments [28, 29]. Thus, sea ice dynamics could potentially help to address the model biases by reducing the amount of too-thick multi-year sea ice present in the model. Also, representing sea ice in PlaSim-LSG in more detail for multi-millennial simulations of past climate could help to reveal the role of sea ice as an important moderating and tipping component in the onset and development of centennial- to millennial scale climate oscillations.

Here, we present our work integrating sea ice dynamics into PlaSim-LSG. While it is essential for more complex GCMs to represent the dynamics of sea ice, this is less common for simplified GCMs or earth system models of intermediate complexity used for coupled simulations of multiple millennia. We describe the pre-existing model configuration, and its newly extended capabilities for dynamic sea ice modelling in Section 2. While one of the primary motivations for these extensions to PlaSim-LSG comes from prospective multi-millennial paleoclimate simulations, we present and discuss initial simulations with the current state of the extended model under present-day climate conditions (Section 3.1). We choose present-day climate for initially constraining the extended model, because direct sea ice observations are available in this period. We test the impact of several key parameters of the sea ice dynamics component (Section 3.2), and evaluate the performance of the new model configuration (Section 3.3). We conclude with future perspectives in Section 4.

2 MODEL DESCRIPTION

2.1 Planet Simulator

PlaSim in version 17 is a simplified GCM which solves the wet primitive equations of the atmosphere in its dynamical core PUMA. We employ a T42 spectral resolution in this study (about 2.8° × 2.8°) and a vertical discretization of 10 layers. PlaSim performs calculations which are for example associated with the mixed-layer ocean, sea ice thermodynamics, and the surface energy balance on a 64 latitude × 128 longitude Gaussian grid [13–15, 20].

The thermodynamic sea ice model in PlaSim is based on the zero-layer Semtner [30] model which is used as well in several other GCMs like the MITgcm [31]. Other than in the standard version of PlaSim-LSG, snow on sea ice is represented following the description of snow on land in the appendix of Andres and Tarasov [20]. In addition to the configuration described there, we implement a simple representation of snow-covered ice, bare ice (meaning ice that is directly exposed to the atmosphere and not covered by snow), and melt pond fraction following the version 2 scheme for sea ice albedo of Køltzow [32]. The purpose of these extensions is to represent the sub-grid scale effects of melt ponds and snow cover on sea ice albedo and the surface energy balance [e.g. 28], which was not the case in PlaSim-LSG previously. We further introduce a globally conservative treatment of excess thermodynamic sea ice growth beyond the physical limits of the sea ice thickness parametrisation in the zero-layer model to improve model stability.

LSG is a 3d general circulation ocean model running at 2.5°× 5° horizontal resolution with 22 vertical layers [16, 22]. LSG implicitly solves the oceanic primitive equations assuming large spatial and temporal scales. This makes a longer integration step than for all other components in PlaSim possible. However, this benefit comes at the expense of not representing gravity waves and barotropic Rossby waves in the ocean [22]. While we run PlaSim at a time step of 20 minutes, one integration step of LSG is performed every 10 days. A mixed-layer ocean with a thickness of 50 m is coupled between LSG and the rest of PlaSim, allowing the ocean to respond to phenomena on shorter time scales than the LSG step. The mixed-layer ocean relaxes to the LSG solution under stationary atmospheric conditions, and mixes the solution from LSG and the thermal response to surface forcing when atmospheric conditions vary [described e.g. in 20].

PlaSim has been coupled to another ocean model, yielding the PlaSim-GENIE model [33]. This implementation replaced the thermodynamic sea ice component of PlaSim and the LSG ocean model by the GOLDSTEINSEAICE and GOLDSTEINOCEAN components. To represent sea ice dynamics, this model employs an advection scheme and uses Laplacian diffusion [34]. Conversely, we choose to retain the LSG model and extend PlaSim-LSG with a component to model sea ice dynamics which we adapt from the MITgcm [31, 35] (see Section 2.2). Unlike PlaSim-GENIE, this approach allows us to also resolve nonlinear viscous-plastic rheologies of sea ice. Another reason is that PlaSim-LSG is user-friendly, well-documented, and extensively studied. Finally, the LSG model has previously been shown to exhibit abrupt climate oscillations [36]. This makes it an ideal test-bed to study such oscillations during the Last Glacial Period.

2.2 Sea ice dynamics component

To model the dynamics of sea ice, we adapt those parts of the MITgcm's sea ice component [35] which solve the sea ice momentum equations of a variant of the nonlinear viscous-plastic (VP) sea ice model introduced by Hibler [37]. The momentum equations in the MITgcm's component are solved with the line-successive-over-relaxation (LSOR) method of Zhang and Hibler

[38] on an Arakawa C grid. Furthermore, we integrate the second- and third-order flux-limited volume- and area-conserving advection schemes from the MITgcm which are used to advect sea ice thickness, concentration, and snow cover [31, 35]. Ice–ocean and ice–atmosphere stresses are directly applied from PlaSim-LSG. While viscous-plastic rheologies with an elliptical yield curve and normal flow rule have been employed for many years in GCMs including MITgcm [e.g. 39, 40], it should be noted that they produce unphysical fracture angles. This is why current development efforts aim at using rheologies which result in better agreements of small-scale sea ice features with observations [e.g. 41, 42]. However, our motivation of incorporating sea ice dynamics into PlaSim-LSG is not to most accurately represent sea ice across a wide range of spatial scales. We rather aim to represent sea ice dynamics in this simplified GCM in sufficient complexity to reduce model biases and study its role in abrupt climate oscillations, which can be observed in multi-millennial simulations with the model. For this purpose, a well-tested and widely-applied sea ice component with elliptical yield curve is sufficient and affordable in terms of added computational costs.

To handle the coupling and interpolation between PlaSim's Gaussian grid and the Arakawa C grid of the dynamic sea ice component, we add and test an intermediate module. We use the pre-existing coupler of PlaSim and LSG to first interpolate any additionally needed oceanic fields to the PlaSim grid. In this process we extend the parallelization architecture of PlaSim to allow for fast handling of neighbouring grid areas used in the discretisations of the sea ice model ("halo exchange"). Additionally, we modify the MITgcm routine interfaces to match with the coding conventions of PlaSim where needed.

In the coupled model, the dynamic sea ice component is called sequentially in every step of PlaSim, with the oceanic stress forcing from LSG being updated at every LSG time step. Thickness categories used in the dynamic model are still represented as zero-layer in the thermodynamic component. This is the default option for the MITgcm sea ice model as well. Given the potential for substantial biases in zero-layer thermodynamic sea ice models, the MITgcm provides an option for the 3-layer model of Winton [43]. This is not available in our configuration due to the current implementation of sea ice thermodynamics in PlaSim.

3 PRELIMINARY RESULTS AND DISCUSSION

3.1 Impact on climatological model biases and simulated climate variability

Starting with the default PlaSim-LSG model parameter set and default parameter settings of the sea ice dynamics component, we run equilibrium simulations under present-day boundary conditions and radiative forcing (CO_2 concentration-equivalent of 360 ppm). Following an initial spin-up phase into a quasi-equilibrium state, we study climatologies over 70 years (150 for the control simulation with only thermodynamic sea ice). Compared to the model setup with only thermodynamic sea ice, we find a strongly decreased mean sea ice extent throughout the year for the model configuration which includes the new component for sea ice dynamics in both hemispheres. Fig. 1 shows this bias for Antarctica. Sea ice extent is below the 1981-2010 median observations for all months. As a result, the 2m temperature has a positive bias compared to reanalysis data (Fig. 2), strongly overcompensating the negative polar 2m temperature bias of the control simulation in the Northern High Latitudes but doing so only slightly in Antarctica. This may hint at the need for differing parametrisations of sea ice albedo for the two hemispheres.

Over all seasons, the mean sea ice thickness from the simulation with the extended model is greatly reduced compared to the configuration with only thermodynamic sea ice in most of the Antarctic Ocean, with thicker accumulations only in the Weddell Sea and Ross Sea (Fig. 1).

We observe a similar behaviour with greatly reduced sea ice thicknesses in the Arctic region (not shown). The configuration with only thermodynamic sea ice exhibits unrealistically thick sea ice under present-day conditions in parts of Antarctica and the Arctic. Thus, tuning of the coupled model should allow us to reach a realistic sea ice state in between the extremes of the configuration of PlaSim-LSG with only thermodynamic sea ice and the extended model.

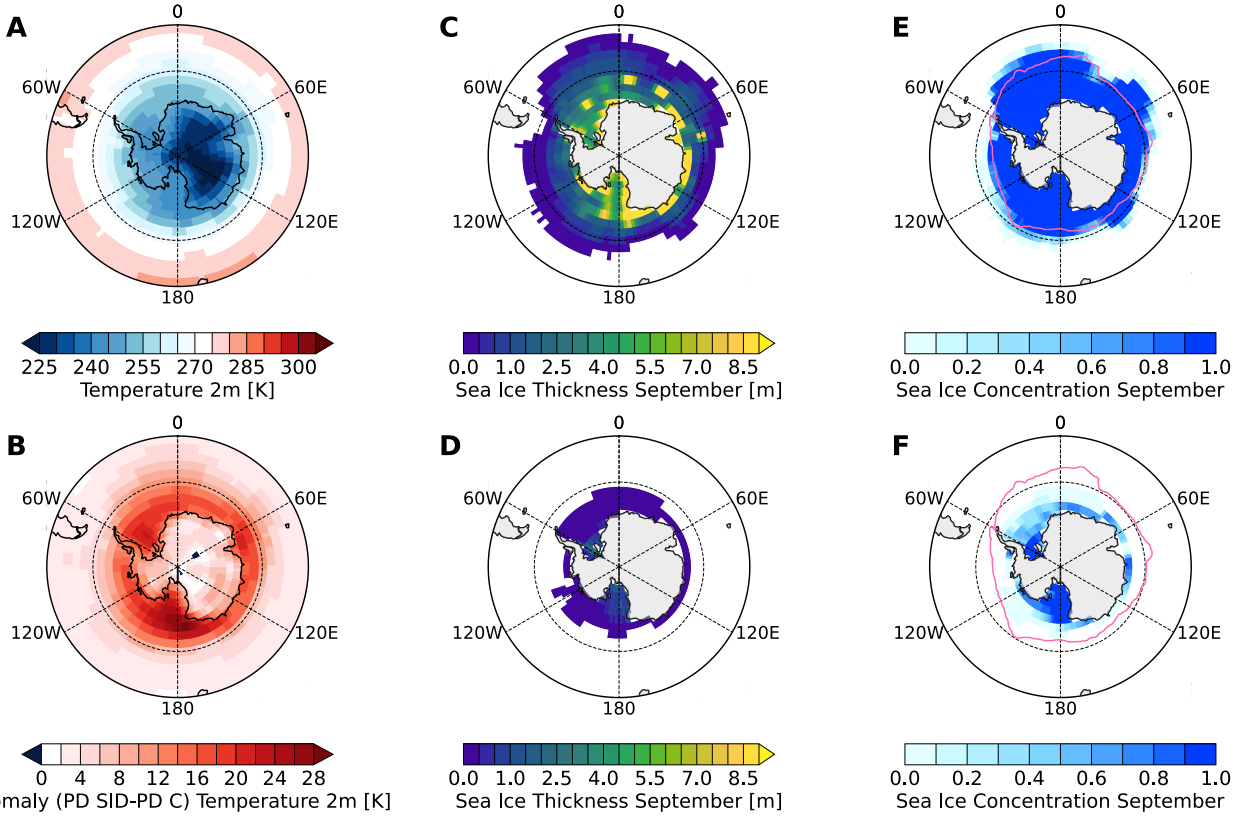

Figure 1: Climatogies of PlaSim-LSG for the present day control simulation (PD C) with only thermodynamic sea ice (top row) and for the simulation with sea ice dynamics under present-day conditions and using the default parametrizations (PD SID, bottom row). Panels show annual mean 2m-temperature of the standard configuration (**A**), annual mean 2m-temperature anomaly between the two configurations (simulation with sea ice dynamics minus control simulation, **B**), absolute sea ice thickness in September (**C, D**) and absolute sea ice concentration in September (**E, F**). The 1981-2010 median sea ice extent of September is indicated in magenta using the data of Cavalieri et al. [44].

Compared to reanalysis data, the model configuration with only thermodynamic sea ice overestimates mid to high latitude annual 2m temperature variability, measured in units of absolute 2m temperature standard deviation of the zonal 2m temperature average (Fig. 2). Conversely, the extended model with sea ice dynamics underestimates 2m temperature variability in Northern mid- to high latitudes. This negative bias in the temperature variability is a lot smaller in Southern mid-latitudes and remains positive for Southern high latitudes. Reduced temperature variability in a state with low amounts of sea ice is in line with previous findings which indicate that temperature anomalies could be amplified less under global warming scenarios which go along with major reductions in sea ice cover [45]. As for the biases of the mean temperature and sea ice states, the results for temperature variability are promising for achieving a realistic representation in between the extremes of the configurations with only thermodynamic sea ice and the one with sea ice dynamics through tuning.

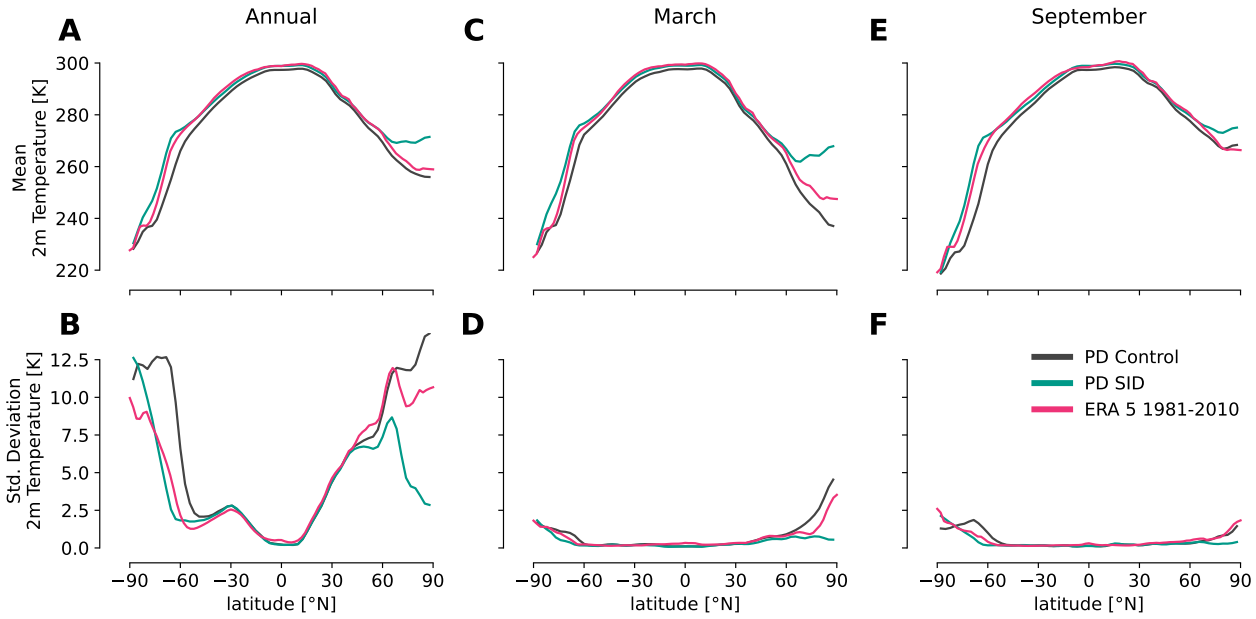

Figure 2: Zonal mean 2m-temperature (top row) and standard deviation (bottom row) for the entire annual cycle (panels A and B), and for monthly climatologies of March (panels C and D) and September (panels E and F) of the present-day control simulation (PD Control), the simulation with sea ice dynamics using default parameters (PD SID), and ERA 5 Reanalysis [46].

3.2 Effects of tuning

We conduct initial tests towards a more realistic representation of sea ice cover in the extended model. Therefore, we vary individual parameters of the dynamic sea ice component aiming at increases in mean sea ice extent, concentration and thickness distribution in the coupled model setup. We only consider key parameters of the sea ice dynamics component and do not conduct a comprehensive tuning procedure involving the entire coupled model. Table 1 lists these parameters which are related to the internal sea ice dynamics or the coupling to oceanic and atmospheric stresses. Parameters are varied equally in both hemispheres to test the general response of the coupled model. The purpose of these initial parameter tests is to gain an understanding for how the coupled model responds to parameter changes in the first place and to provide a basis for more systematic parameter tuning.

Overall we find little to no impact for individual parameter changes in 30 year-averaged simulation data. Sea ice concentration and thickness are slightly increased when changing the sea ice strength parameter P^* to $P^* = 3.1625 \times 10^4\,\mathrm{N/m^3}$ compared to the default parameters. P^* (see Table 1) is the main free parameter in the sea ice strength parametrization, which is why it is particularly suited for modifications [37]. The most notable impact can be found in and around the Beaufort Sea and East Siberian Sea in the Arctic (Fig. 3). For the Antarctic, sea ice extent and concentration are still generally too low. Thus, more realistic values cannot be achieved by variations in individual parameters of the sea ice component alone. Evaluating combinations of varied parameters at once and involving the thermodynamic sea ice component, the albedo parametrisation, and other components of the coupled model in a more rigorous process of parameter optimisation are possible next steps to improve the tuning of PlaSim, following e.g. Mehling et al. [47]. In addition, different parameterisations for the two hemispheres might need to be considered in the tuning. This is generally supported by previous findings indicating that the most accurate representations of sea ice by models which

Table 1: Main parameters related to the sea ice-internal dynamics, and to the coupling to ocean and atmosphere which can be subject to model tuning.

Parameter [units]	Variable name	Description	Default value	Tested values
C_w [10^{-3}]	`SEAICE_waterDrag`	Water drag for freely drifting sea ice	5.5	1.1, 2.4, 3.5, 6.2 (See Table 1 in [49] and the findings of [50])
k_2 [N/m^3]	`SEAICEbasalDragK2`	Parameter and implicit flag for basal stress parametrisation of landfast sea ice	0.0	15.0 (see [51] for additional parameters u_0, k_1, k_2 which have not been changed from defaults here)
C^* [1]	`SEAICE_cStar`	Empirical (exponential) scaling constant to couple sea ice thickness and strength following [37]	20.0	Not changed, same impact achievable with parameter P^*
P^* [10^4 N/m^3]	`SEAICE_strength`	Primary free parameter to couple sea ice thickness and strength following [37]	2.75	2.61, 2.89, 3.025, 3.1625 (correspond to $\sim \pm 5\%$ steps from MITgcm default)
κ [1]	`SEAICEstressFactor`	Overall coupling factor of sea ice and wind stress to ocean surface layer	1.0	0.9, 0.95, 1.05

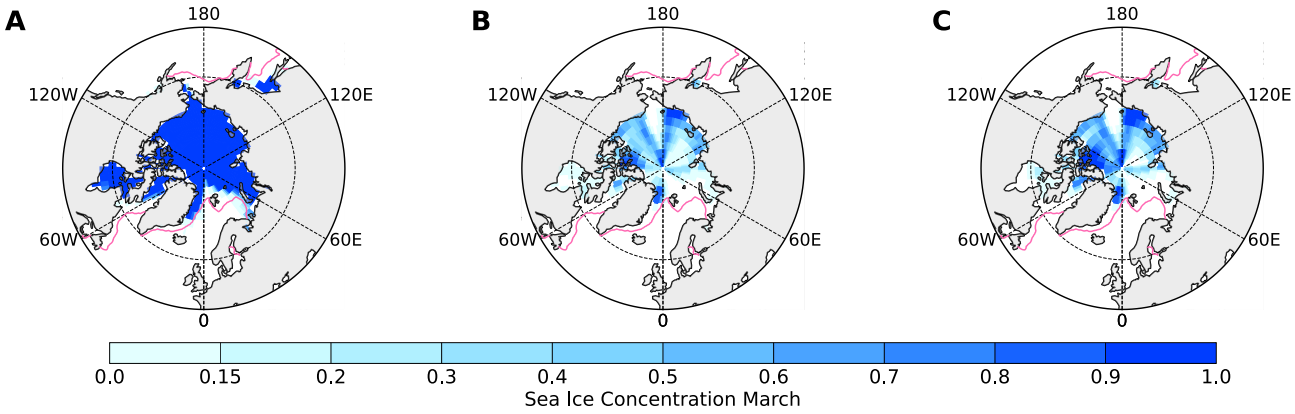

Figure 3: Sea ice concentration and extent in March for the PlaSim-LSG model with only thermodynamic sea ice (panel **A**), the default parametrisation of the extended model with sea ice dynamics (parameter $P^* = 2.75 \times 10^4\,\mathrm{N/m^3}$, **B**), and with an increased parameter $P^* = 3.1625 \times 10^4\,\mathrm{N/m^3}$ (**C**). The 1981-2010 median sea ice extent of March is indicated in magenta using the data of Cavalieri et al. [44].

comprise a VP rheology with an elliptical yield curve cannot be achieved with a single global value of the sea ice strength parameter [48]. A limiting factor for high values of P^* are the potentially inaccurate representations of small-scale sea ice features [42], which are, however, not the focus of our effort of representing sea ice dynamics in this simplified GCM used for multi-millennial simulations of past climate.

3.3 Model Performance

We compare the performance of the new model configuration to the different possible configurations of PlaSim-LSG and the core model PlaSim, for the hardware capabilities of a standard server (Intel Core i5-8600K, $6 \times 3.60 - 4.30\,\mathrm{GHz}$, simulations in this study on 4 cores) and a general purpose high performance computing cluster. Table 2 shows the total run time and the resulting simulation times achievable per day of simulation. The added component increases the simulation time per year by about 10 % compared to the standard PlaSim-LSG setup. For a T42 resolution we achieve a decent benefit when increasing the number of computing cores from eight to sixteen (35 % speed-up). Further increase to 32 cores does only decrease run time marginally. This hints at the primary limitation of performance of PlaSim-LSG in general. In the current implementation the LSG ocean component is not parallelized, although

it is sequentially coupled.

Table 2: Typical computational cost of different model setups. If not stated otherwise, the given numbers refer to a coupled PlaSim-LSG setup with only thermodynamic sea ice at T42 resolution (see Section 2).

Machine	Core Number and Clock Rate [GHz]	Time per simulation year [mn]	Simulation years per day
Standard Server	4×4.3	$\simeq 13.0$	111
Standard Server (with sea ice dynamics)	4×4.3	$\simeq 14.2$	101
Standard Server (only PlaSim core model)	2×4.3	$\simeq 6.4$	225
Standard Server (only PlaSim core model, T21)	2×4.3	$\simeq 2.7$	533
General purpose cluster	8×2.1 (0.25 node)	$\simeq 12.0$	122
General purpose cluster	16×2.1 (0.5 node)	$\simeq 7.8$	184
General purpose cluster	32×2.1 (1 node)	$\simeq 7.2$	199

4 CONCLUSION

We extended the simplified general circulation model PlaSim-LSG with a component for sea ice dynamics adapted from the MITgcm. While it is essential for state–of–the–art general circulation models to represent the coupled dynamics of sea ice, it is less common for simplified general circulation models, which are used for multi-millennial simulations of the past climate, to feature sea ice dynamics. The component now added to PlaSim-LSG solves the Hibler [37] sea ice momentum equations with a non-linear viscous-plastic rheology, and advects sea ice as a response to stress forcing, thereby adopting the most common representation of sea ice dynamics in more complex general circulation models. We studied climatological biases of 2m-temperature, and sea ice extent and thickness in the PlaSim-LSG configuration with only thermodynamic sea ice and with the new model extension under present-day climate conditions. The extended model presently under-represents sea ice extent and thickness compared to present-day observations, and exhibits ice-free summer months. Through this, the negative temperature bias of the standard model configuration in mid- to high latitudes is overcompensated. As expected, the reduced amount of sea ice leads to decreased temperature variability in mid- to high latitudes compared to the PlaSim-LSG version without thermodynamic sea ice. Thus, sea ice dynamics is of great importance for the mean state and variability of the high-latitude climate simulated by PlaSim-LSG.

Variations of individual parameters of the sea ice dynamics component have small to negligible impact on the sea ice bias of the extended model. More thorough tuning of the coupled model components simultaneously is required. However, while the extended model underestimates sea ice thickness and extent, the configuration with only thermodynamic sea ice overestimates them. Therefore we expect that a realistic present-day state in between these extremes can be reached through appropriate and comprehensive tuning of the coupled model. Introducing different parametrisations for the two hemispheres into the dynamic and thermodynamic sea ice components could provide an additional possibility to improve the simulated climate of the model.

Modelling sea ice dynamics adds about 10 % of runtime to the PlaSim-LSG model. This is reasonable given the comparably high degree of explicit formulations introduced into the model architecture to represent sea ice dynamics in more detail. The main bottleneck of the PlaSim-LSG combination remains the unparallelized LSG ocean component, which limits effective parallelization to sixteen cores. While additional tests for physical consistency, model stability under varying boundary conditions, and tuning remain, the extended model adds to the repertoire of different PlaSim-LSG configurations and allows us to study the impact of sea

ice dynamics on known biases of the model. Given the reasonable computational effort needed to run the extended model, it can potentially contribute to the understanding of mechanisms which led to past climate oscillations in multi-millennial simulations of the Last Glacial Cycle.

CODE AVAILABILITY

The most recent state of the extended model can be accessed on GitHub: https://www.github.com/paleovar/plasim17sid.

ACKNOWLEDGEMENTS

This research has been funded by the Deutsche Forschungsgemeinschaft (DFG, German Research Foundation), project no. 395588486, and contributes to the PalMod project (https://www.palmod.de). The German Academic Scholarship Foundation (Studienstiftung) funded the stay of MA at Memorial University. We thank one anonymous reviewer for their valuable comments on the manuscript. MA thanks Lev Tarasov for enabling the research stay at Memorial University. We thank Frank Lunkeit for helpful discussions around the PlaSim-LSG model, Lev Tarasov for discussions on integrating the new sea ice component, and Elisa Ziegler for valuable comments on the manuscript. We acknowledge support by the state of Baden-Württemberg through bwHPC for computations on the bwUniCluster (https://www.bwhpc.de). We thank the MITgcm developers for making their extensively documented model code available. The NSIDC data on sea ice extent was downloaded from https://nsidc.org/data/seaice_index/archives (last access: 15.05.2021). The ERA5 surface temperature data was downloaded from the Copernicus Climate Data Store (last access: 19.04.2020).

REFERENCES

[1] P. Braconnot et al. *Nature Climate Change* 2 (2012), 417–424. DOI: 10.1038/nclimate1456.
[2] G. A. Schmidt et al. *Climate of the Past* 10.1 (2014), 221–250. DOI: 10.5194/cp-10-221-2014.
[3] C. Li et al. *Journal of Climate* 23.20 (2010), 5457 –5475. DOI: 10.1175/2010JCLI3409.1.
[4] A. Voigt and D. S. Abbot. *Climate of the Past* 8.6 (2012), 2079–2092. DOI: 10.5194/cp-8-2079-2012.
[5] G. Vettoretti and W. R. Peltier. *Geophysical Research Letters* 43.10 (2016), 5336–5344. DOI: 10.1002/2016GL068891.
[6] C. Li and A. Born. *Quaternary Science Reviews* 203 (2019), 1 –20. DOI: 10.1016/j.quascirev.2018.10.031.
[7] T. M. Dokken et al. *Paleoceanography* 28.3 (2013), 491–502. DOI: 10.1002/palo.20042.
[8] U. Hoff et al. *Nature Communications* 7.1 (2016), 12247. DOI: 10.1038/ncomms12247.
[9] G. Flato et al. *Climate Change 2013: The Physical Science Basis. Contribution of Working Group I to the Fifth Assessment Report of the Intergovernmental Panel on Climate Change*. Ed. by T. Stocker et al. Cambridge, United Kingdom and New York, NY, USA: Cambridge University Press, 2013.
[10] T. Hajima et al. *Progress in Earth and Planetary Science* 1.1 (2014), 1–25. DOI: 10.1186/s40645-014-0029-y.
[11] M. Claussen et al. *Climate Dynamics* 18.7 (2002), 579–586. DOI: 10.1007/s00382-001-0200-1.
[12] H. Goosse et al. *Geoscientific Model Development* 3.2 (2010), 603–633. DOI: 10.5194/gmd-3-603-2010.
[13] K. Fraedrich et al. *Meteorol. Z.* 14.3 (2005), 299–304. DOI: 10.1127/0941-2948/2005/0043.
[14] F. Lunkeit et al. Tech. rep. 2012. URL: https://www.mi.uni-hamburg.de/en/arbeitsgruppen/theoretische-meteorologie/modelle/sources/psusersguide.pdf.
[15] F. Lunkeit et al. Tech. rep. 2012. URL: https://www.mi.uni-hamburg.de/en/arbeitsgruppen/theoretische-meteorologie/modelle/sources/psreferencemanual-1.pdf.
[16] E. Maier-Reimer and U. Mikolajewicz. Tech. rep. Max-Planck-Institut fuer Meteorologie Hamburg, 1992. DOI: 10.2312/WDCC/DKRZ_Report_No02.
[17] F. Lunkeit. *Chaos* 11.1 (2001), 47–51. DOI: 10.1063/1.1338127.
[18] K. Fraedrich. *European Physical Journal Plus* 127.5 (2012). DOI: 10.1140/epjp/i2012-12053-7.
[19] G. Margazoglou et al. *Proceedings of the Royal Society A* 477.2250 (2021), 20210019. DOI: 10.1098/rspa.2021.0019. eprint: 2010.10374.
[20] H. J. Andres and L. Tarasov. *Climate of the Past* 15.4 (2019), 1621–1646. DOI: 10.5194/cp-15-1621-2019.

[21] C. Covey et al. *Global and Planetary Change* 37.1-2 (2003), 103–133. DOI: 10.1016/S0921-8181(02)00193-5.
[22] E. Maier-Reimer et al. *Journal of Physical Oceanography* 23.4 (1993), 731–757. DOI: 10.1175/1520-0485(1993)023⟨0731:MCOTHL⟩2.0.CO;2.
[23] F. Feser et al. *Theoretical and Applied Climatology* 65.1-2 (2000), 1–15. DOI: 10.1007/s007040050001.
[24] P. Braconnot et al. November (2004), 515–533. DOI: 10.1007/978-1-4020-2121-3_24.
[25] A. M. McCabe et al. *Science* 325.5941 (2009), 710–714. DOI: 10.1126/science.1172873.
[26] E. Ziegler et al. EGU General Assembly 2021, online, 19–30 Apr 2021, EGU21-11006, 2021. DOI: 10.5194/egusphere-egu21-11006.
[27] H. Andres and L. Tarasov. EGU General Assembly 2021, online, 19–30 Apr 2021, EGU21-13778, 2021. DOI: 10.5194/egusphere-egu21-13778.
[28] C. Haas. *Sea Ice: An Introduction to its Physics, Chemistry, Biology and Geology*. Ed. by D. N. Thomas and G. S. Dieckmann. Blackwell Science Ltd, 2003.
[29] J. Zhang and D. Rothrock. *Journal of Geophysical Research: Oceans* 105.C2 (2000), 3325–3338. DOI: 10.1029/1999jc900320.
[30] A. J. Semtner. *Journal of Physical Oceanography* 6.3 (1976), 379 –389. DOI: 10.1175/1520-0485(1976)006⟨0379:AMFTTG⟩2.0.CO;2.
[31] MITgcm Group. Last accessed: 14.10.2021. MIT/EAPS, Cambridge, MA 02139, USA, 1997-2021. URL: https://mitgcm.readthedocs.io/en/latest/.
[32] M. Køltzow. *Journal of Geophysical Research: Atmospheres* 112.D7 (2007). DOI: 10.1029/2006JD007693.
[33] P. B. Holden et al. *Geoscientific Model Development* 9.9 (2016), 3347–3361. DOI: 10.5194/gmd-9-3347-2016.
[34] N. R. Edwards and R. Marsh. *Climate Dynamics* 24.4 (2005), 415–433. DOI: 10.1007/s00382-004-0508-8.
[35] M. Losch et al. *Ocean Model.* 33.1-2 (2010), 129–144. DOI: 10.1016/j.ocemod.2009.12.008.
[36] G. Knorr and G. Lohmann. *Geochemistry, Geophysics, Geosystems* 8.12 (2007). DOI: 10.1029/2007GC001604.
[37] W. D. Hibler. *Journal of Physical Oceanography* 9.4 (1979), 815–846. DOI: 10.1175/1520-0485(1979)009⟨0815:adtsim⟩2.0.co;2.
[38] J. Zhang and W. D. Hibler. *Journal of Geophysical Research* 102.4 (1997), 412–415. DOI: 10.1029/96JC03744.
[39] D. Ferreira et al. *Journal of Climate* 24.4 (2011), 992–1012. DOI: 10.1175/2010JCLI3580.1.
[40] F. Zheng et al. *Advances in Atmospheric Sciences* 38.1 (2021), 29–48. DOI: 10.1007/s00376-020-9223-6.
[41] D. Ringeisen et al. *Cryosphere* 15.6 (2021), 2873–2888.
[42] A. Bouchat and B. Tremblay. *Journal of Geophysical Research: Oceans* 122.7 (2017), 5802–5825. DOI: 10.1002/2017JC013020.
[43] M. Winton. *Journal of Atmospheric and Oceanic Technology* 17.4 (2000), 525 –531. DOI: 10.1175/1520-0426(2000)017⟨0525:ARTLSI⟩2.0.CO;2.
[44] D. J. Cavalieri et al. Last accessed: 19.05.2021. Boulder, Colorado USA. NSIDC: National Snow and Ice Data Center, 1996, updated yearly. DOI: 10.5067/8GQ8LZQVL0VL.
[45] C. Huntingford et al. *Nature* 500.7462 (2013), 327–330. DOI: 10.1038/nature12310.
[46] H. Hersbach et al. *Quarterly Journal of the Royal Meteorological Society* 146.730 (2020), 1999–2049. DOI: 10.1002/qj.3803.
[47] O. Mehling et al. EGU General Assembly 2021, online, 19–30 Apr 2021, EGU21-1328, 2021. DOI: 10.5194/egusphere-egu21-1328.
[48] S. Juricke et al. *Journal of Climate* 26.11 (2013), 3785–3802. DOI: 10.1175/JCLI-D-12-00388.1.
[49] P. Lu et al. *Journal of Geophysical Research: Oceans* 116.C7 (2011). DOI: 10.1029/2010JC006878.
[50] H. D. B. S. Heorton et al. *Journal of Geophysical Research: Oceans* 124.8 (2019), 6388–6413. DOI: 10.1029/2018JC014881.
[51] J.-F. Lemieux et al. *Journal of Geophysical Research: Oceans* 120.4 (2015), 3157–3173. DOI: 10.1002/2014JC010678.